ICMGP 2024
CAPE TOWN • SOUTH AFRICA • 21 - 26 JULY

ECNU

Improved mechanistic modeling on reproducing particle-bound mercury in the marine atmosphere

Long Chen, Yanping Zhang, Zeng Xu, Guitao Shi, Xuejun Wang

East China Normal University
chenlong@geo.ecnu.edu.cn

Outline

- ☐ Introduction
- ☐ Methods and materials
- ☐ Results and discussion
- ☐ Conclusion

Hg

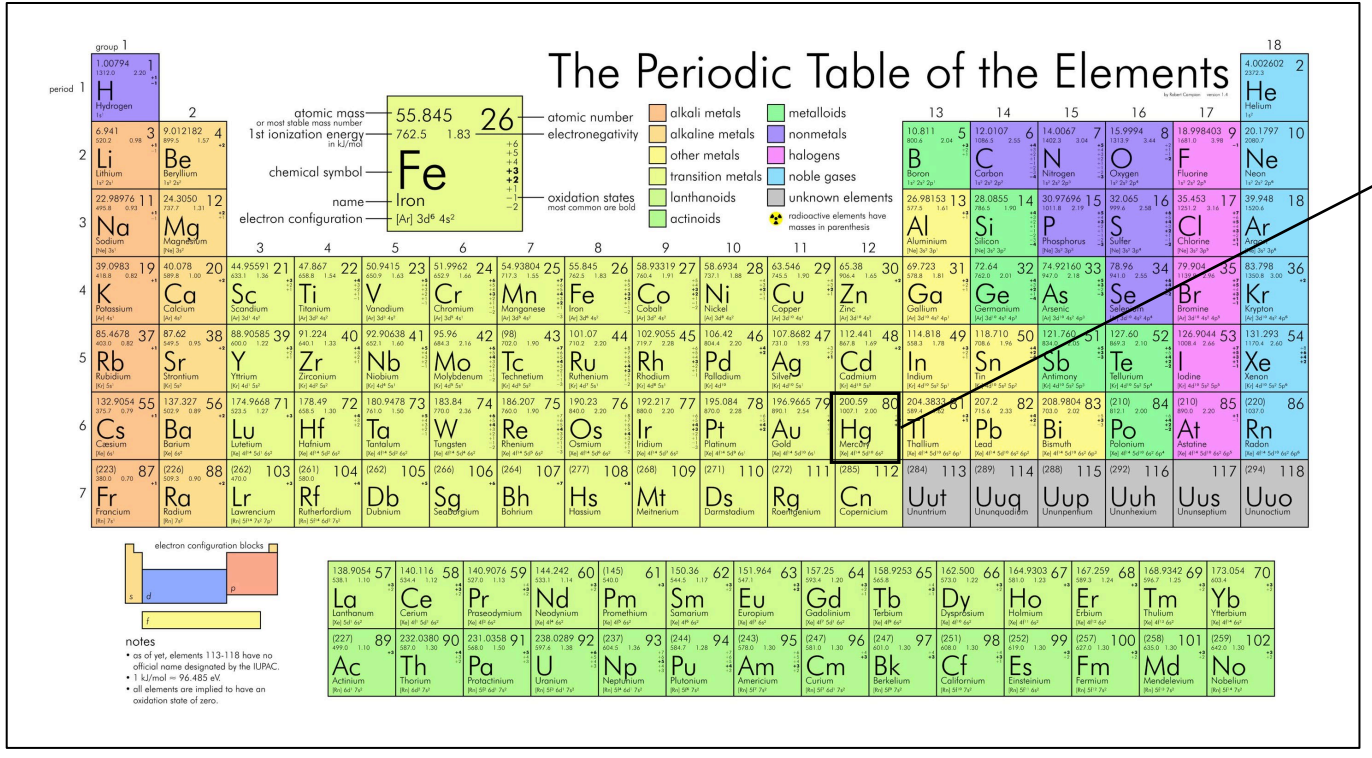

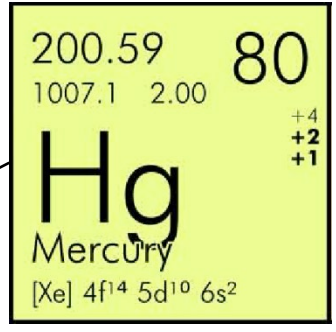

Hg^0 Hg^{2+} Hg^P

Ubiquitous on the planet!

Hg cycling and health impacts

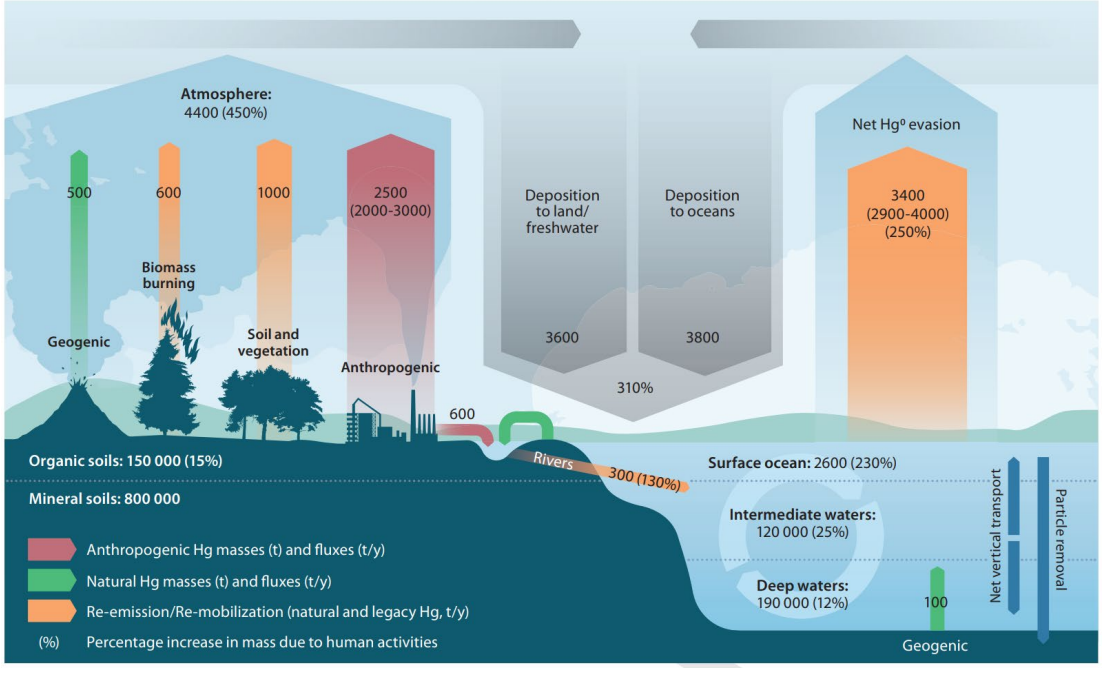

UN Environment (2019)

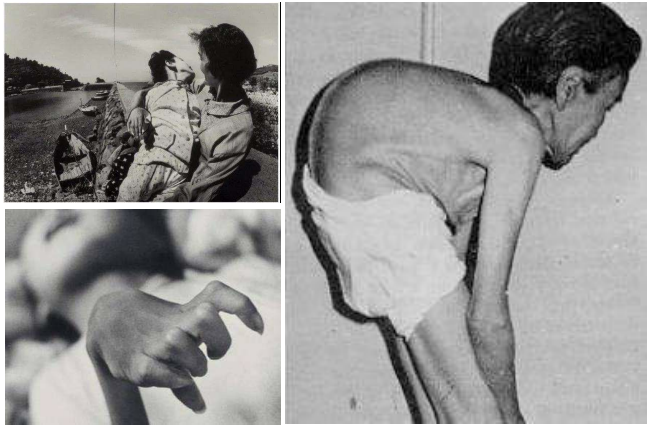

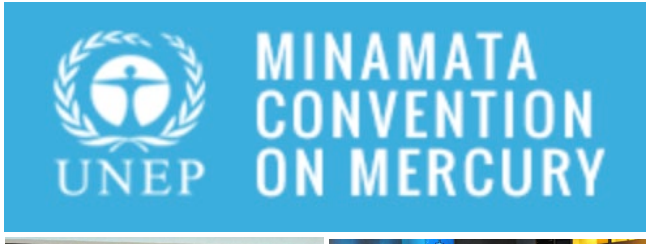

Hg^P formation and importance

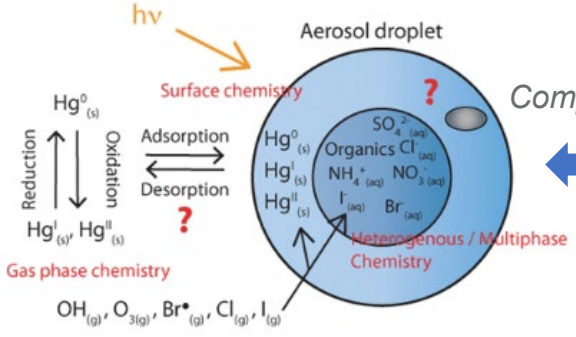

(Ariya et al., 2015)

Competitive

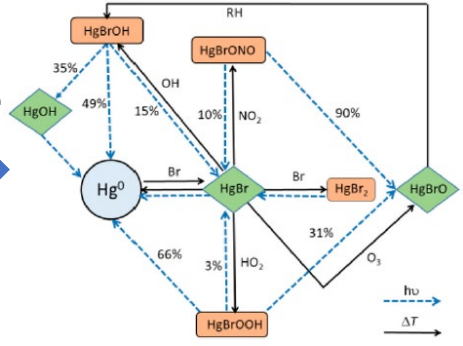

(Saiz-Lopez et al., 2018, 2020)

SSA-bound Hg^P

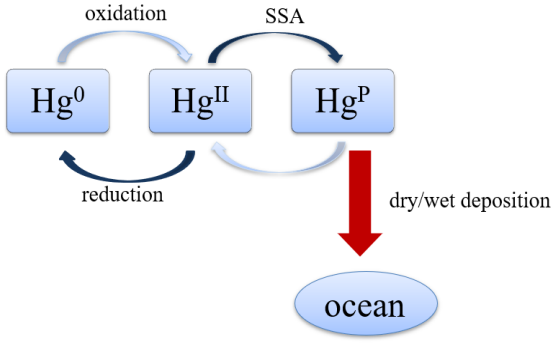

The formation of Hg^P stems mainly from the adsorption of Hg^{II} on aerosol particles such as **nitrate**, **sulfate**, and **sea salt aerosols (SSA)**

Rapid gaseous photoreduction of Hg^{II} to Hg^0

Hg^P formation is also a critical process that exacerbates Hg deposition and subsequent potential risks on the planet

Modeling Hg^P formation in global models

- Statistics-based schemes

$$K_P = \frac{[PBM]}{[PM_{2.5}][GOM]}$$

$$\log(1/K_P) = a + \frac{b}{T}$$

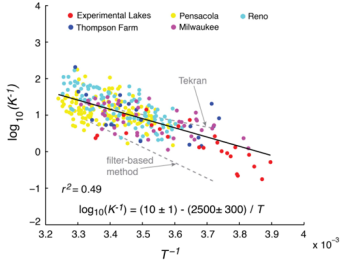

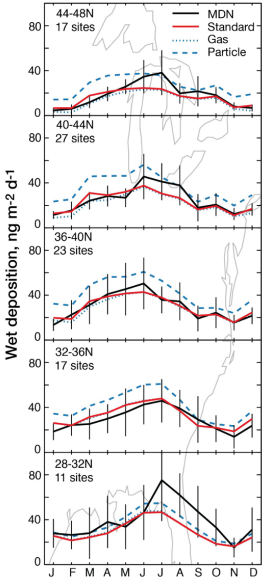

Good performance over the continents

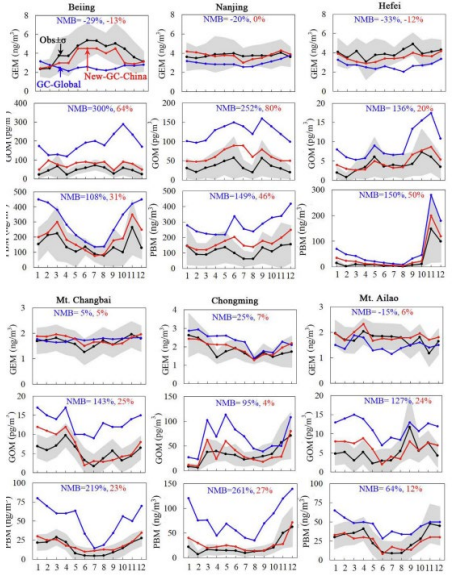

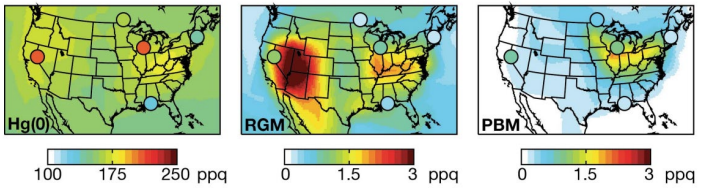

Table 2 – Hg^{II} gas-particle partitioning relationship in New-GC-China.

Region	RH	OA	Hg^{II} gas-particle partitioning	Sites
Eastern coastal grids below 10 m a.s.l.	/	/	$\log(1/K_P) = -(1200\pm170)/T + (5 \pm 1)$	Chongming
Inland areas	RH< 60%	/	$\log(1/K_P) = -(2700\pm280)/T + (10\pm1)$	Beijing Nanjing
Inland areas	60%≤RH≤80%	/	$\log(1/K_P) = -(2100\pm230)/T + (8 \pm 1)$	
Inland areas	RH>80%	<8 μg/m^3	$\log(K_P) = 0.25\times\log[OA] - 1.00$	
Inland areas	RH>80%	≥8 μg/m^3	$\text{Log}(K_P) = -1.14\times\log[OA] + 0.25$	

(Amos et al., 2012; Liu et al., 2022)

Modeling Hg^P formation in global models

- Statistics-based schemes

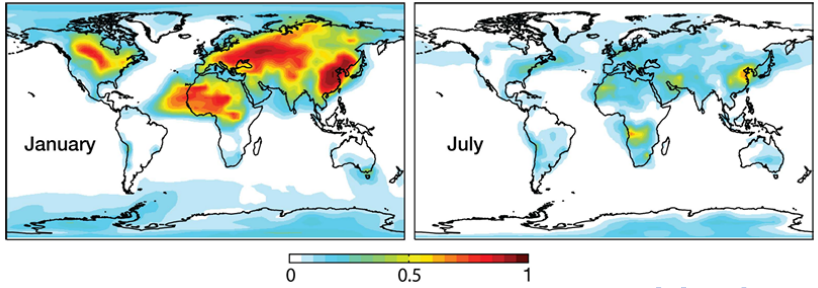

$Hg^{II}/(Hg^{II}+Hg^P)$

Underestimate!

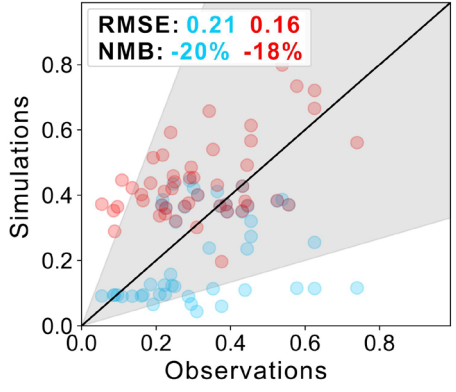

How about the performance over the ocean?

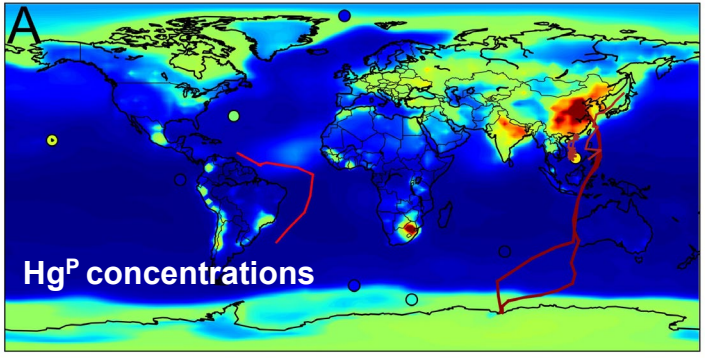

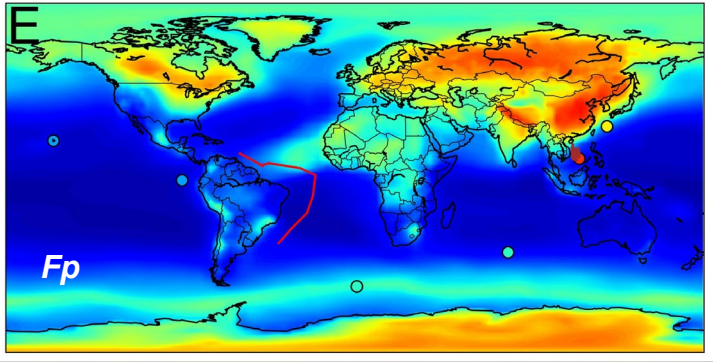

$Fp = Hg^P/(Hg^{II}+Hg^P)$

- GEOS-Chem (v14.1.1) Hg modeling

  (Shah et al., 2021; Feinberg et al., 2022)

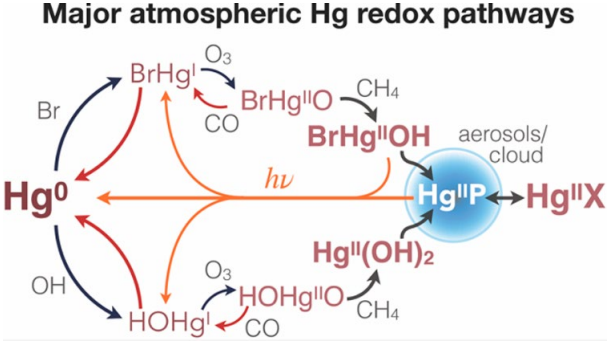

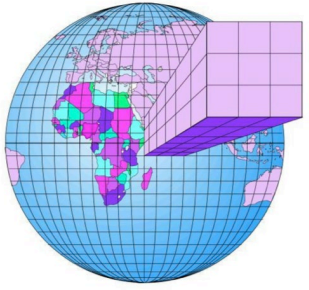

- Anthropogenic inventory with long-term Hg emissions

  Streets et al., 2019: 2000-2015

  Scaling based on CO_2 emissions (ODIAC): 2016-2023

- Long-term simulations (2008–2023) at latitude 2° × longitude 2.5° horizontal resolution

Process-based schemes

Hygroscopic growth of sea salt particles

$$r = r_{dry}\frac{4}{3.7}\left(\frac{2-S}{1-S}\right)^{1/3}$$

$$\rho_{wet} = \left(\rho r_{dry}^3 + \rho_{H_2O}(r^3 - r_{dry}^3)\right)/r^3$$

Adsorption of Hg^{II} on the particles

$$k_{mt} = \frac{4\pi r^2}{L}\left(\frac{r}{D_g} + \frac{4}{v\alpha}\right)^{-1}N$$ Mass transfer rate

$$J = Lk_{mt}\left(C - \frac{C_a}{H}\right)$$ Concentration gradients

$$\frac{d_{C_{a,i}}}{dt} = \frac{J_i}{L_i} - v_{d,i}\frac{C_{a,i}}{Z}$$

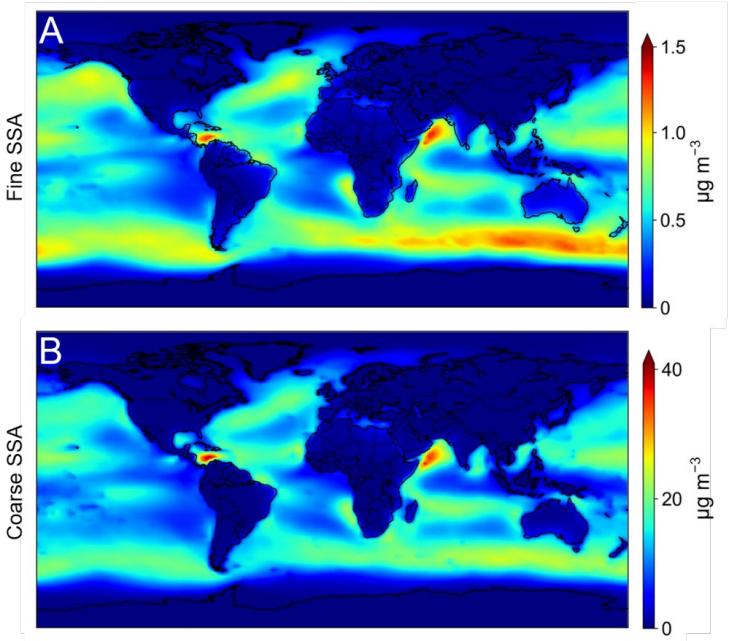

Nine bins of dry radii ranging from 0.01 to 8 μm were established in this study in accordance with Fan et al. (2011): **0.01–0.2, 0.2–0.4, 0.4–0.6, 0.6–0.8, 0.8–1, 1–2, 2–4, 4–6, and 6–8 μm**

Atmospheric Hg observations

Inland/Coastal observations

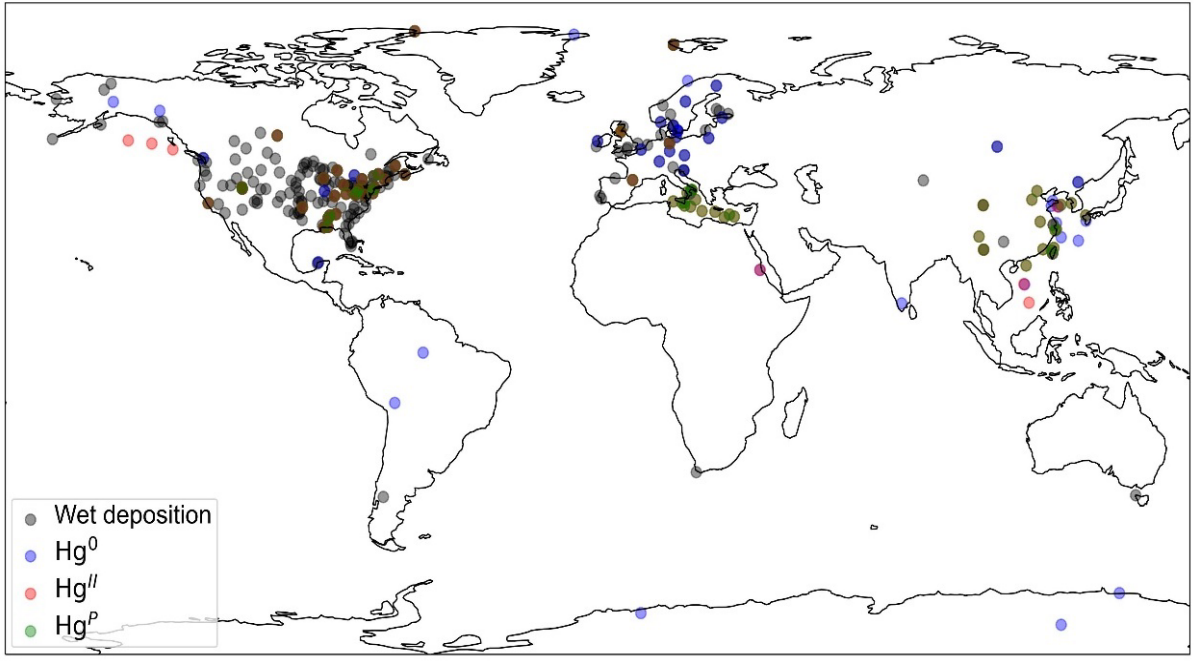

- CAPMoN
- AMNet
- EMEP
- GMOS
- MDN
- Literature data

Atmospheric Hg observations

☐ Marine observations from offshore islands and cruises

- **Five ship cruises** across the ocean:
  South Atlantic Ocean
  West Pacific Ocean
  Weddell Sea
  North Atlantic Ocean
  Southern Ocean

- **Five offshore islands:**
  Hawaii islands
  Bermuda
  Amsterdam Island
  The Galápagos islands
  Taiping Island

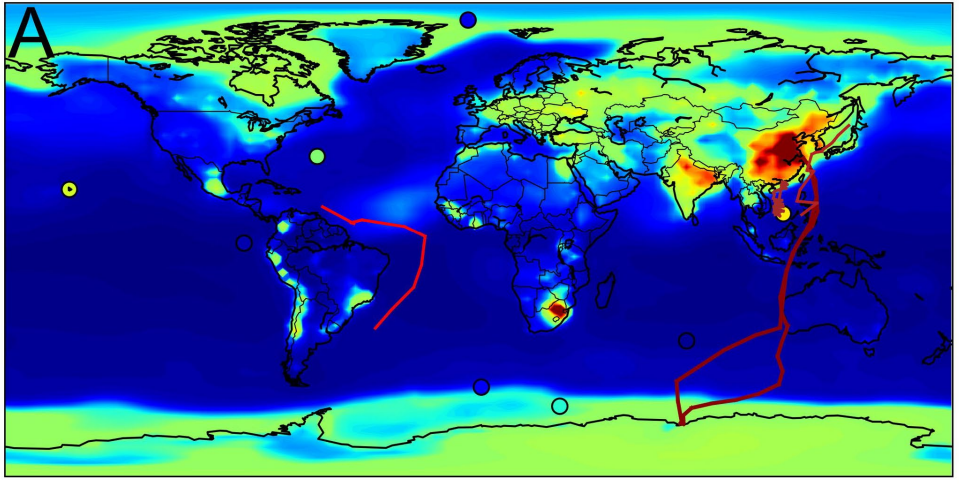

Correction of atmospheric Hg^{II} concentrations

- Numerous studies have reported the underestimation of Hg^{II} concentrations measured by KCl-coated denuders from the widely-used Tekran speciation systems, and the factors of underestimation ranged from **1.3 to 13**

- A median value of **2.4** was used to correct the observations of Hg^{II} concentrations in this study, and the median value has been observed for the measuring efficiency of cation exchange membranes (CEM) over KCl-coated denuders on collecting $HgCl_2$, which is the main component of Hg^{II} in the atmosphere

Model performance on Hg^0 and Hg^{II} concentrations

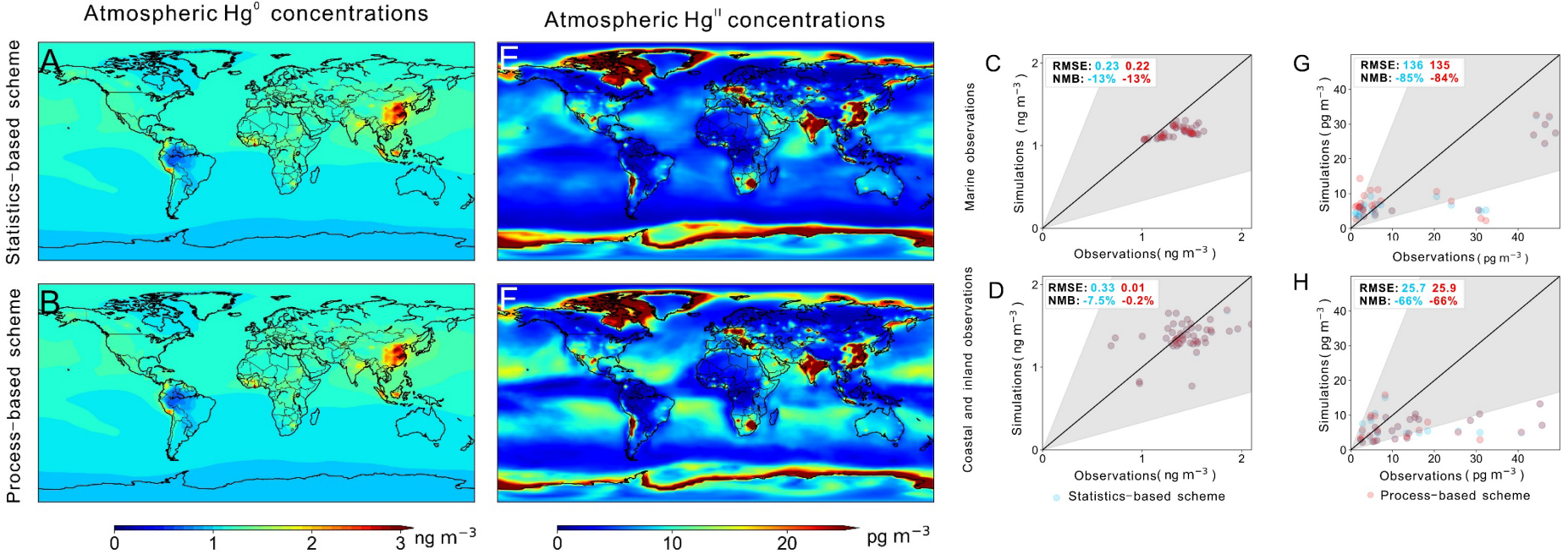

- Good performance on Hg^0 and Hg^{II} simulations
- Insignificant difference of the performance between these two schemes

Reproducing Hg^P concentrations and F_p in the marine atmosphere

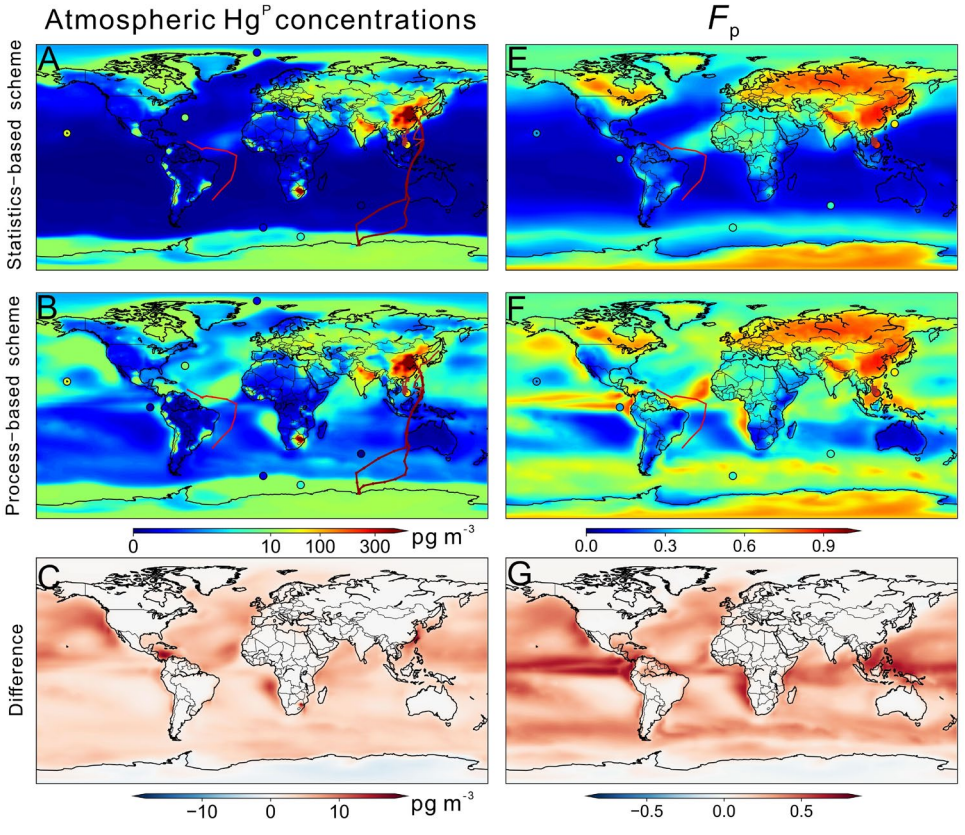

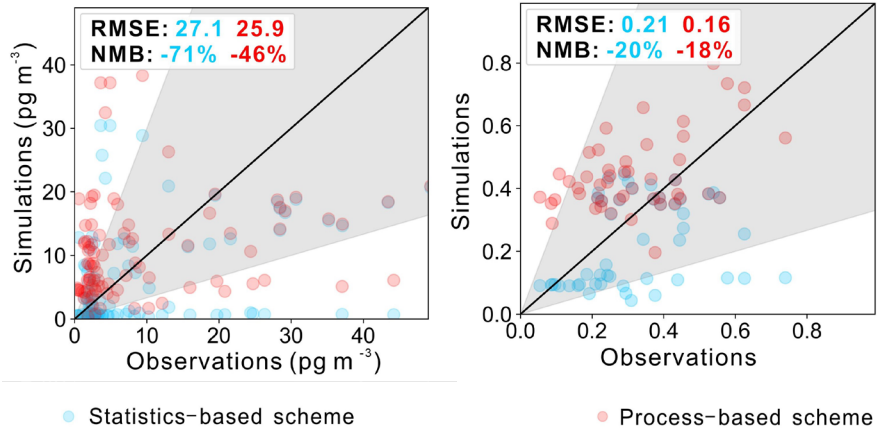

- Significantly improve the model performance on Hg^P cycling in the marine atmosphere using the process-based scheme

Remaining Hg^P concentrations and F_p in the continental atmosphere

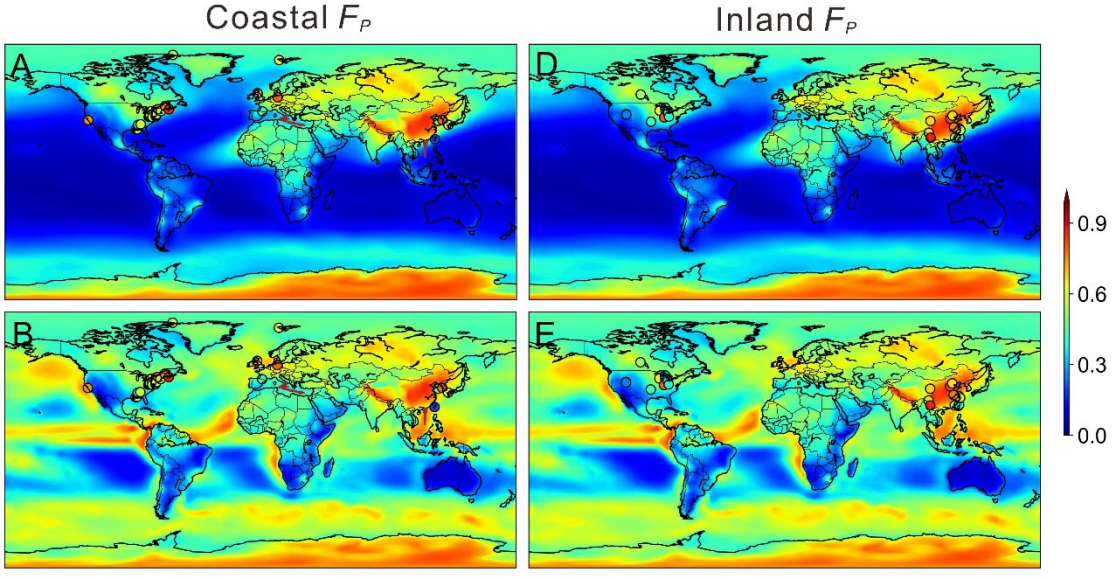

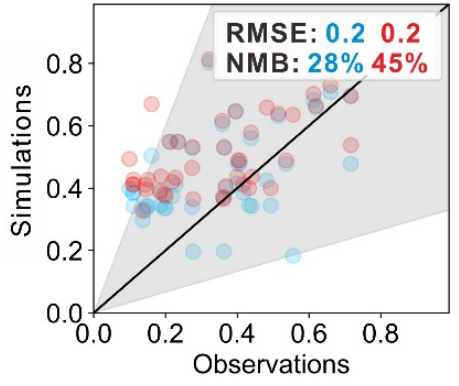

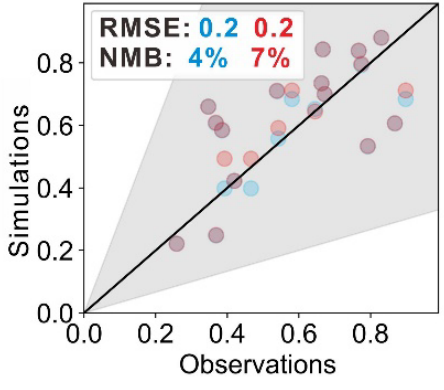

Insignificant difference of the performance between these two schemes

Improved model performance on wet deposition over the ocean

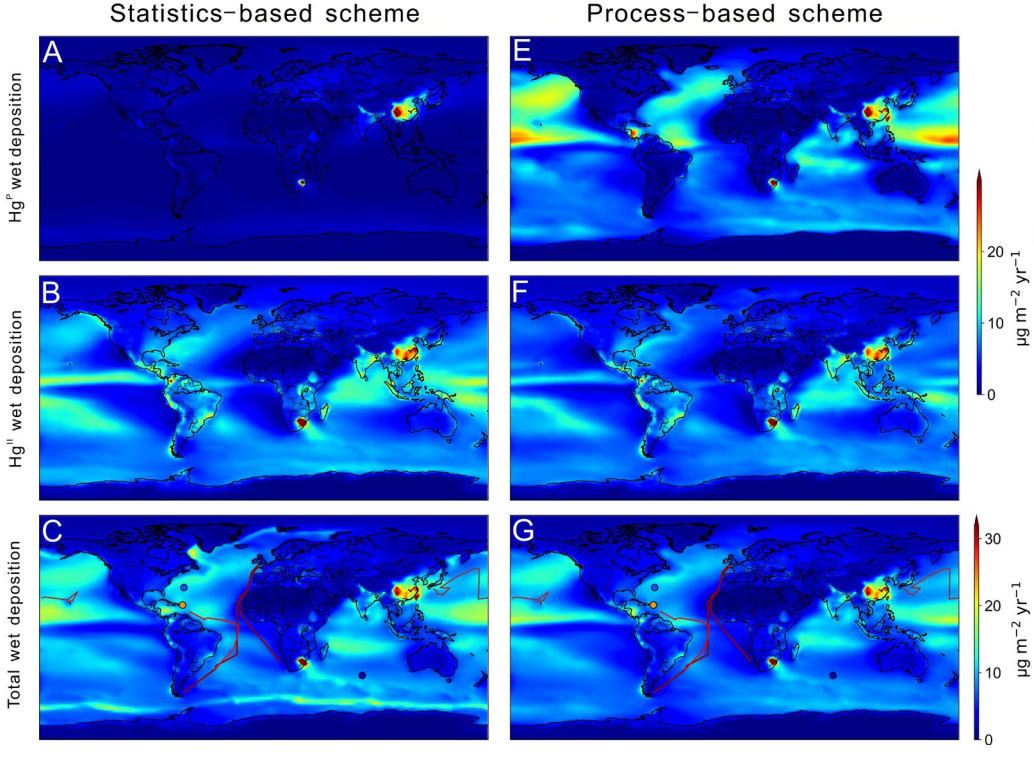

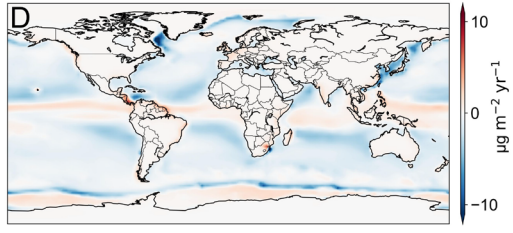

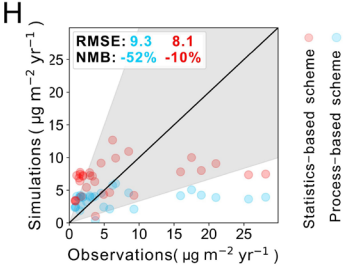

- The reconstruction of atmospheric Hg^P by the process-based scheme evidently contributed to the observed increase in Hg^P wet deposition, but the decrease in Hg^{II} wet deposition over the ocean compared to the statistics-based scheme

- Total wet deposition with the sum of Hg^P and Hg^{II} showed a similar spatial distribution between the two schemes

Global distribution of size-resolved sea salt aerosol-bound Hg^P

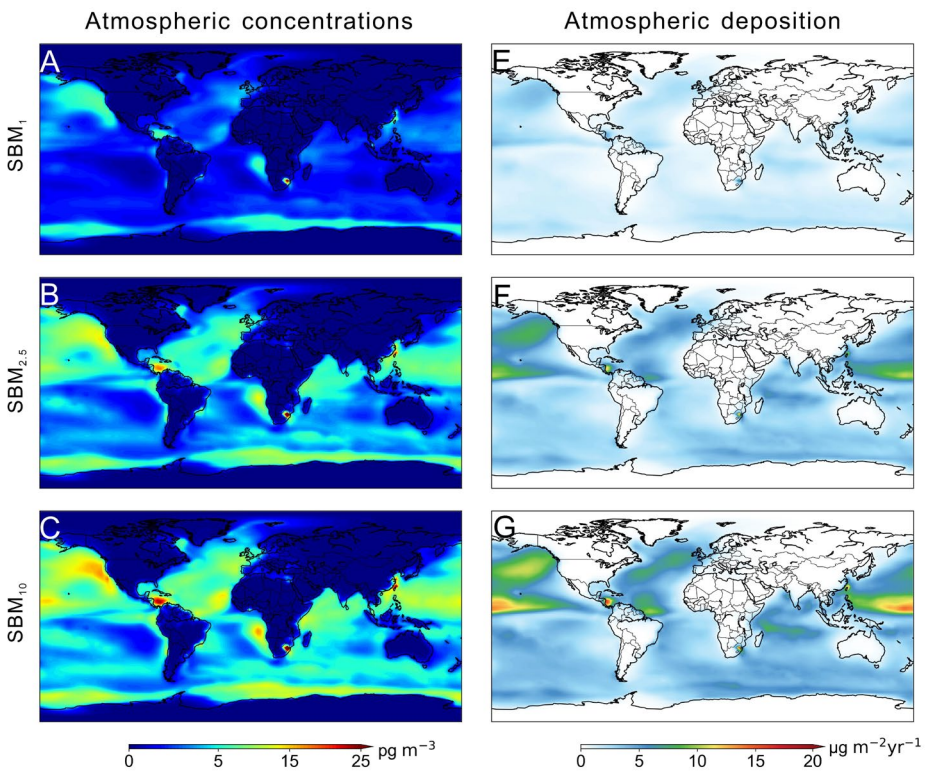

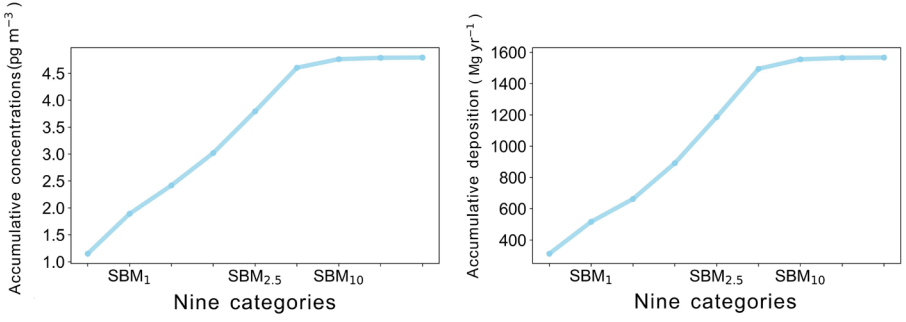

- Atmospheric concentrations and annual deposition flux of SBM_1 were much lower than those of $SBM_{2.5}$ and SBM_{10}, and the magnitudes of $SBM_{2.5}$ and SBM_{10} were comparable
- Hotspots were observed over Northern Hemisphere waters, such as the North Pacific and North Atlantic
- The global total deposition fluxes of SBM_1, $SBM_{2.5}$, and SBM_{10} were estimated to be **515 Mg yr^{-1}**, **1,145 Mg yr^{-1}**, and **1,550 Mg yr^{-1}** respectively, accounting for **33.0%**, **75.7%**, and **99.3%** respectively.

Implications for global atmospheric mercury budget

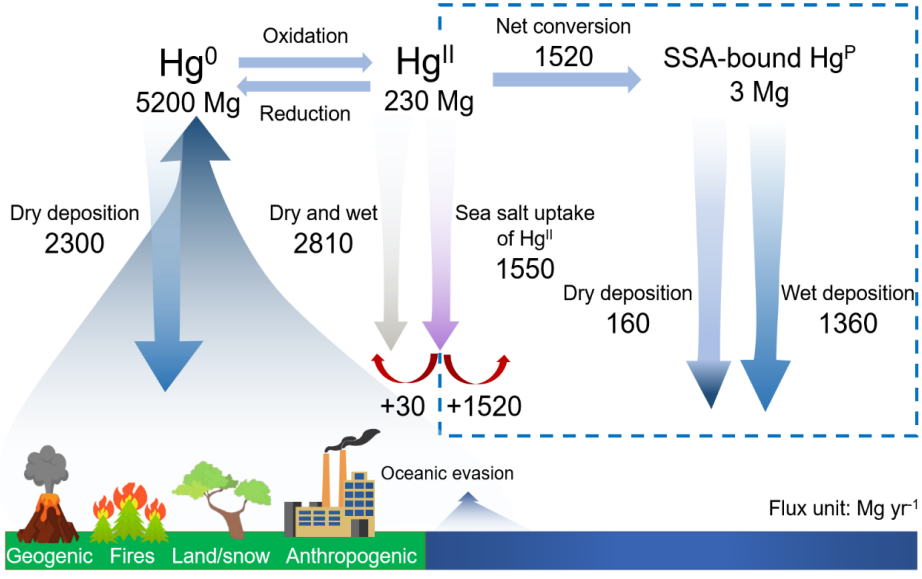

- The major change of the new budget was the **transition** from gaseous Hg^{II} deposition to particulate Hg^{P} deposition over the ocean

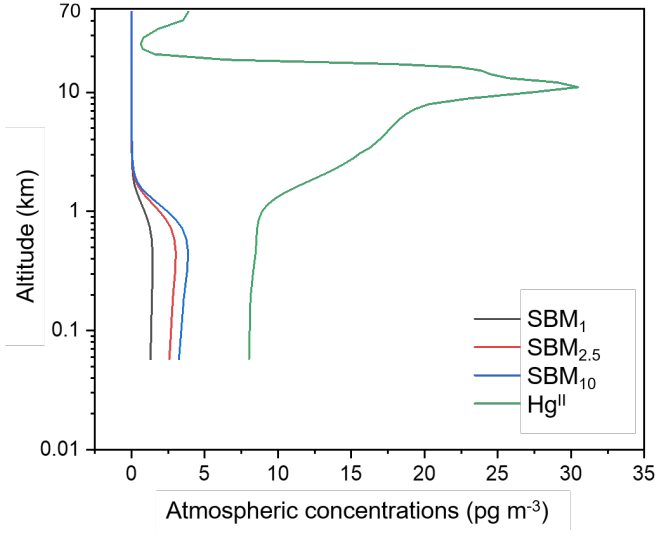

- The atmospheric burden of SSA-bound Hg^{P} was low (3 Mg), because the formation of SSA-bound Hg^{P} occurred mainly in air columns with limited height

*Zhang, **Chen***, … et al., In revision*

- The process-based scheme reproduced Hg^P concentrations and F_p in the marine atmosphere

- A new global atmospheric Hg cycling budget was constructed that accounted for the SSA-bound Hg^P cycling in the marine atmosphere. The major change of the new budget was the **transition** from gaseous Hg^{II} deposition to particulate Hg^P deposition over the ocean

- Atmospheric burden of SSA-bound Hg^P was low (3 Mg), because the formation of SSA-bound Hg^P occurred mainly in air columns with limited height

THANKS!

This research was supported by the National Natural Science Foundation of China (42077200)